APPLIED MATERIALS AND TECHNOLOGY

Jamt.ejournal.unri.ac.id

Research Article

Characterization and impact of graphene oxide on the curing and mechanical properties of epoxy resins

Gina Maritzell Colmenares Jimenez*, Adhimar Flávio Oliveira, Tessa Martins de Carvalho Carneiro, Estacio Tavares Wanderley Neto, Maria Elena Leyva Gonzalez

ABSTRACT: Graphene oxide (GO) has been widely studied as a nanofiller for epoxy resins due to its excellent mechanical, thermal, and interfacial properties. In this study, GO was synthesized via electrochemical exfoliation and characterized using FTIR, XRD, TGA, and SEM. GO was incorporated into an epoxy matrix (Litestone 3200 resin with 2131H hardener) at different weight percentages (0.10%, 0.13%, 0.20%, and 0.50%), and the curing behavior was analyzed through differential scanning calorimetry (DSC). The cure kinetics were evaluated using the Kissinger and Ozawa methods. The results indicated that the activation energy increased at 0.13% GO but decreased at higher concentrations. TGA analysis showed that the addition of GO improved thermal stability, particularly at 0.10% GO. FTIR confirmed the presence of oxygenated functional groups in GO, XRD indicated partial exfoliation and structural disorder, and SEM revealed sheet-like morphology. These results were consistent and complementary, supporting the successful incorporation of GO into the epoxy network. The addition of GO slightly improved the mechanical modulus without significantly altering the glass transition temperature (Tg).

Keywords: *Graphene oxide, Epoxy resin, Curing kinetics, Mechanical properties, Thermal stability*

1. INTRODUCTION

Epoxy composites have gained prominence in the industry due to their excellent mechanical, thermal, and chemical properties, making them widely used in construction, aerospace, automotive, and electronic applications [1, 2]. However, the growing demand for high-performance materials with reduced environmental impact has driven the development of novel composites, particularly those reinforced with nanostructured materials such as graphene oxide (GO).

To better contextualize this approach, we highlight below the properties and previous studies involving GO-epoxy composites. Graphene oxide (GO) has emerged as a promising nanofiller for epoxy resins due to its high surface area, oxygen-containing functional groups, and good compatibility with polar matrices. These characteristics enhance interfacial adhesion and facilitate improved mechanical and thermal properties in epoxy-based nanocomposites [3,4]. The hydroxyl, epoxy, and carboxyl groups on the GO surface interact with the epoxy matrix during curing, promoting stronger interfacial bonding and potential changes in the cure kinetics [5].

Several studies have demonstrated that incorporating GO into epoxy resins, even at low concentrations, can enhance both thermal and mechanical performance. Zhang et al. [6] reported increased tensile strength and decomposition temperature in GO/epoxy systems at 0.1–0.3 wt%. Similarly, Liu et al. [7] found that GO promoted faster curing and improved crosslink density due to its functionalized surface acting as a catalyst and nucleation agent. These studies support the use of GO as an effective modifier for multifunctional epoxy composites.

OPEN ACCESS

Affiliation
Universidade Federal de Itajubá, Av BPS, 1303, Pinheirinho, Itajubá, MG 37500-903, Brasil.

***Correspondence**
Email: gina.colmenaresjimenez@gmail.com

ORCID
Jimenez, G., M., C.: 0009-0001-4773-113X
Oliveira, A., F.: 0000-0003-2586-7359
Carneiro, T., M., C.: 0009-0009-9392-9567
Neto, E., T., W.: 0000-0002-1241-7378
Gonzalez, M., E., L.: 0000-0003-0673-5713

Received: June 07, 2025
Revised: July 06, 2025
Accepted: July 10, 2025

How to cite: Jimenez, G., M., C., Oliveira, A., F., Carneiro, T., M., Neto, E., T., W., Gonzalez, M., E., L. (2025). Characterization and impact of graphene oxide on the curing and mechanical properties of epoxy resins. *Journal of Applied Materials and Technology*, 7(1), 11–21. https://doi.org/10.31258/Jamt.7.1.11-21.

While GO is widely studied, fewer investigations focus specifically on electrochemically exfoliated GO and its effect on epoxy systems. Compared to the Hummers' method, electrochemical exfoliation offers GO with fewer impurities, thinner sheets, and higher functionalization [8]. These characteristics may enhance its interaction with the resin matrix. Therefore, this study aims to evaluate how different concentrations of electrochemically exfoliated GO influence the curing kinetics, glass transition temperature (Tg), thermal stability, and mechanical behavior of epoxy composites.

GO, a derivative of graphene, exhibits unique characteristics, including a high surface area-to-volume ratio, the presence of oxygen-containing functional groups, and good dispersibility in polymeric matrices [9,10]. These properties make GO an excellent modifier for epoxy matrices, potentially enhancing their mechanical strength, thermal stability, and even imparting new functionalities, such as electrical conductivity and improved chemical resistance [11].

A critical aspect of developing GO-reinforced epoxy composites is understanding the cure kinetics of the system. The curing process directly influences the final properties of the material, and its investigation allows for the optimization of processing conditions and material performance. Kinetic analysis can be performed using various models, such as the Kissinger, Ozawa, and Flynn-Wall-Ozawa (FWO) methods, which enable the determination of Arrhenius parameters, including activation energy (E) and pre-exponential factor (A0) [12]. The Kissinger method is one of the most widely used approaches and is based on the following equation:

$$ln\left(\frac{\beta}{T_p^2}\right) = -\frac{E}{RT_P} + ln\left(\frac{AR}{E}\right) \quad (1)$$

where β is the heating rate, Tp is the peak transition temperature, R is the universal gas constant, and E is the activation energy [13]. This method allows for the calculation of the activation energy by plotting $ln\left(\frac{\beta}{T_p^2}\right)$ versus $\frac{1}{T_P}$, from which the slope can be used to determine E.

The Ozawa method provides an alternative analysis by utilizing the equation:

$$ln\,\phi = -\frac{E}{RT} - ln\,A_0 \quad (2)$$

The FWO method, a model-free isoconversional method, is given by:

$$ln\,\beta = -\frac{1.051\,E}{RT_P} + C \quad (3)$$

where C is a constant for a given conversion level. This method enables the estimation of the activation energy at different degrees of conversion without presuming a particular kinetic model [14]. Together, these methods provide a comprehensive understanding of the cure kinetics, crucial for tailoring the thermal and mechanical properties of GO-reinforced epoxy composites. Thus, this study aims to investigate the cure kinetics of an epoxy resin modified with GO by employing different thermal analysis methods to determine the kinetic parameters. The obtained results will enable the evaluation of how GO incorporation affects the resin's reactivity, contributing to the development of novel epoxy-based composites with enhanced properties and improved processing efficiency. The expected outcomes include a detailed understanding of the effect of GO on the cure kinetics of epoxy resins, facilitating the optimization of processing parameters and broadening their technological applications.

2. MATERIALS AND METHODS

Graphene oxide (GO) used in this work was prepared as reported in a previous article. The materials used were commercial graphite 4390 6B, KOHNOOR HARDTMUTH and concentrated sulfuric acid purchased from NEON Commercial Analytical Reagents LTDA, Brazil. For the fabrication of the composites, Litestone 3200E epoxy resin with Litestone 213H hardener was used. The characteristic data of the Resin and Hardener are presented in Table 1.

Table 1. Characteristic data of Epoxy Resin and Hardener.

Properties	Epoxy Resin Litestone 3200E	Hardener Litestone 21331h
Viscosity at 25°C [mPas] ASTM D445	11000 to 14000	75 - 150
Density at 25°C [g/cm³] ASTM D0452	1.1 - 1.2	1.1 - 1.2
Shelf life (months)	24	12

The product's technical sheet reports that curing is carried out for one hour at 90°C, followed by two hours at 140°C. Table 2 presents the properties of the resin after curing.

Table 2. Properties of the cured system.

Properties	Value
Tg (°C/min) DSC, midpoint, 10K/min	130-140
Tensile Strength [MPa] ASTM D638	90
Young's Modulus [GPa] ASTM D638	3.2
Elongation at peak [%] ASTM D638	5.2
Flexural Strength [MPa] ASTM D790	114
Flexural Modulus [GPa] ASTM D790	2.2

GO was prepared by the electrochemical exfoliation of graphite using an anodic method. The electrolytic cell consisted of graphite block electrodes as the anode and cathode and 0.5 M H_2SO_4 as electrolyte and intercalant. Exfoliation occurred by applying a direct current voltage of +3 V for 10 min, using an Instrutherm power supply, model FA-3005 digital, single channel, voltage up to 32 V, current up to 5 A. Then, the voltage was increased to +5 V for 5 min and subsequently increased to +7 V for another 5 min.

After electrochemical exfoliation, the product was kept in an ultrasonic bath using a Cristofoli ultrasonic cleaner at a frequency of 42 kHz for four hours. Finally, simple filtration was performed and washed with distilled water until reaching neutral pH. The product was dried in a Venticell oven for 24 hours with forced air circulation at a temperature of 100°C. Epoxy resin - graphene oxide composite (ER-GO) was prepared by adding graphene oxide in amounts of 0 wt%, 0.10 wt%, 0.13 wt%, 0.20 wt%, and 0.50 wt%

to the weight of the epoxy resin. The mixed content was stirred for 10 min and then the hardener was added in a ratio of 100:92, 100 parts resin to 92 parts hardener. The beaker contents were poured into silicone molds and cured following the manufacturer's recommendations, one hour at 90°C followed by two hours at 140°C.

For the characterization of graphene oxide and ER-GO composite, various techniques were used: Thermogravimetric Analysis (TGA), X-Ray Diffraction (XRD), Differential Scanning Calorimetry (DSC), Fourier Transform Infrared Spectroscopy (FTIR), Scanning Electron Microscopy (SEM) and Mechanical Testing.

Fourier Transform Infrared - Attenuated Total Reflectance (FTIR-ATR) was used to obtain information about the chemical structure of all samples. The spectra were recorded in the wavenumber range of 650 to 4000 cm^{-1} at 22°C. The analysis was performed using a Shimadzu IRTracer-100 spectrometer, with an average of 32 scans per spectrum and a resolution of $8cm^{-1}$. The microstructure of the GO powder was characterized by X-ray diffraction (XRD). The diffraction patterns were collected using a Malvern Panalytical X'Pert PRO diffractometer equipped with CuK radiation (λ = 1.5406˚A) and a graphite monochromator. The scanning range 2θ was set between 5° and 70° with intervals of 0.02° and a scanning speed of 5.0 s per step. The morphology of all samples was examined using scanning electron microscopy (SEM). A Zeiss EVO MA 15 SEM was used, operating with an acceleration voltage of 15 kV and a working distance (WD) of 16-19mm. The samples were fixed on double-sided carbon tape and were not gold-coated before analysis. TGA measurements were carried out using a TGA-60, Shimadzu, at a constant heating rate of 10°C min^{-1} from 25 to 1000°C under a nitrogen atmosphere (50 mL.min^{-1}). A Shimadzu Model DSC 60 was used to study the cure kinetics of epoxy anhydride systems and to determine the glass transition temperature (Tg) of ER-GO composite networks. Studies on curing kinetics of epoxy resin and GO were carried out by dynamic scans, samples (5mg) were sealed in aluminum pans, and heated between 25 to 250°C at rates of 5°C/min, 10°C/min, 15°C/min and 20°C/min. Glass transition temperatures were investigated in ER-GO composites previously cured. Tg was defined by the onset temperature of the change in specific heat was determined during a subsequent scan at 10°C/min. Mechanical testing was performed by a universal testing machine, EMIC model DL 3000, with a 5.0 kN load cell at 50% relative humidity and 23°C. Tensile properties of ER-GO composites were studied by compressive strength following ASTM 695 standard at 1.0mm/min using cylindrical specimens 10 ± 0.2mm long with 12 ± 0.2mm diameters. The reported values were averaged from measurements of at least five specimens.

3. RESULT AND DISCUSSION

In Figure 1, we present the FTIR spectrum of graphene oxide (GO). The FTIR spectrum shows a broad band between 3740 cm^{-1} and 3500 cm^{-1}, indicating the presence of O-H carboxyl or oxygen functional groups. [15].The vibration band at 1737 cm^{-1} is assigned to the C=O stretching of the carboxyl group (COOH), located at the edges of GO. The stretching vibration at 1076 cm^{-1} corresponds to C-O bond of the hydroxyl and epoxide groups on the basal planes. The vibration band at 1564 cm^{-1} is attributed to C=C bonds of the graphene skeleton [16]. Figure 2 shows the X-ray diffraction plot of graphene oxide obtained in this work. The XDR pattern found is comparable to that reported for the GO ob-

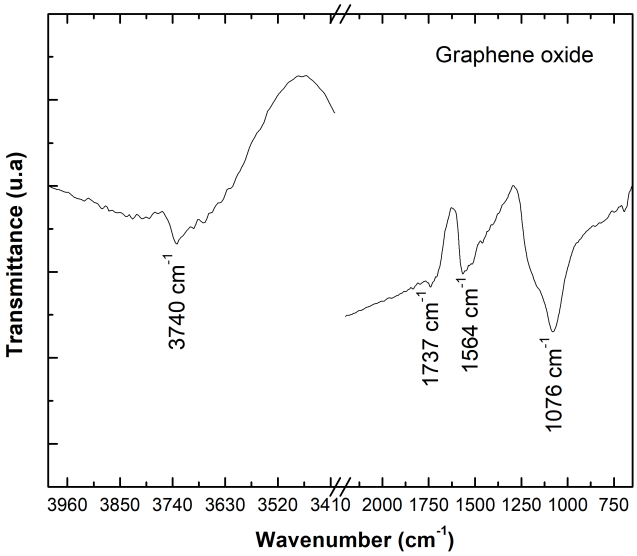

Figure 1. FTIR spectrum of GO.

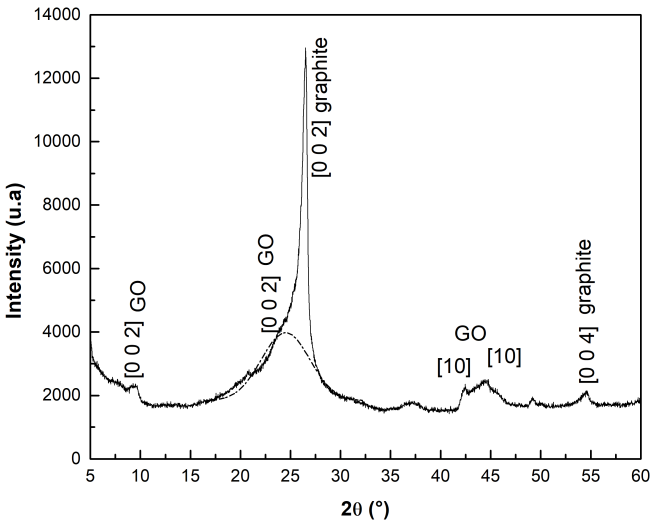

Figure 2. XRD pattern of the obtained GO.

tained by electrochemical exfoliation of graphite [17]. The XRD reveals impurities of graphite (2θ= 26.5°) and the presence of two carbon forms in the GO: one with high (2θ= 9.5°) and the other with low (2θ= 24.5°), concentrations of functional groups.

GO with a high concentration of functional groups exhibits a characteristic peak at the [002] crystalline plane at 9.5°, indicating an increase in interplanar distance due to the introduction of oxygenated groups, such as hydroxyls and epoxides, between the graphene layers. This increased interlayer spacing suggests a higher oxygen content, a characteristic expected in highly oxidized GO samples [18].

On the other hand, GO with a low concentration of functional groups is identified by the broadening of the peak base between 20° and 30°, centered at 24.5°, indicating less distance between graphene layers. The two-dimensional (10) reflection exhibits two diffraction peaks at 2θ = 42.5° and 44.5°, related to short-range order in stacked graphene layers. The characteristic peak at the [002]

Table 3. Interplanar distance and crystallite size of GO.

2θ(°)	β(rad)	d(nm)	H(nm)	n	D(nm)
9,5	0,016	0,93	8,58	9	8,96
24,5	0,017	0,37	1,32	4	-
26,5	0,016	0,34	8,78	75	-
42,5	0,010	0,21	-		29,07
44,5	0,027	0,20	-		11,19

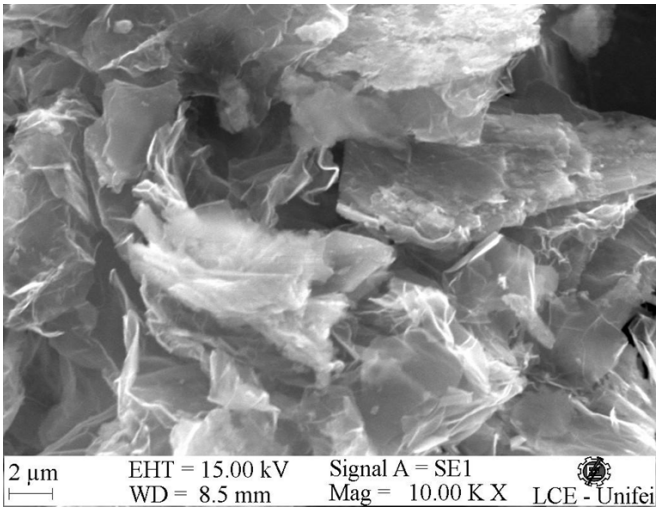

Figure 3. SEM of GO.

crystalline plane at 26.5° is assigned to the graphitic structure, indicating that some regions still retain the crystalline organization of graphite [18]. For the calculation of interplanar distance, we used Bragg's law [19]. The characteristic [002] reflection was used to estimate the graphene flake thicknesses or average height of stacking layers (H) by the Scherrer equation, using a constant equal to 0.9. The average layer numbers (n) can be obtained by the division of the thickness (H) by the interlayer distance (d):

$$n = \left(\frac{H}{d}\right)$$

To estimate the average diameter of stacking layers (D), the Scherrer equation was used with the Warren constant of 1.84 in the diffraction peak related to the two-dimensional (10) reflection [20]. The results obtained for all peaks are presented in Table 3.

Therefore, as we already said, the GO obtained by electrochemical exfoliation of graphite consists of a mixture of different graphene oxides. Nanostructures stacking with an average layer number between 4 to 9 and average diameter between 29.07 nm to 11.19 nm, having impurities of graphite.

Table 3 shows that the interplanar distance for the highly oxidized phase (0.93 nm) was significantly greater than that of the less oxidized phase (0.37 nm), with these values being consistent with those found in the literature [21].

In Figure 3, we present an SEM image of the GO obtained in this study. The presence of GO sheets is observed, indicating that the exfoliation method used was effective. The micrograph reveals wrinkled surfaces at the edges of the sheets, suggesting different degrees of stacking [22].

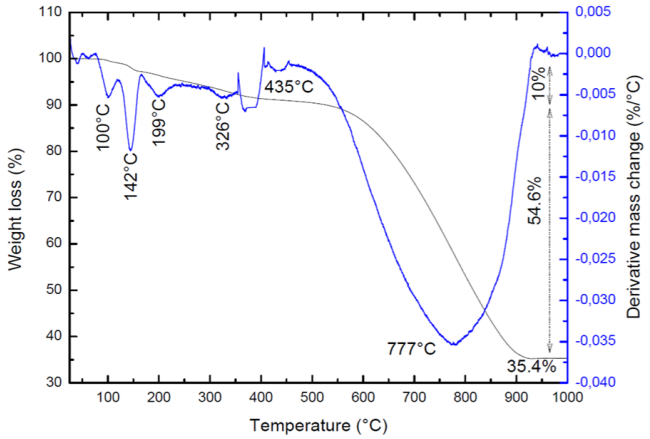

Figure 4. TGA (black row)-DTG (blue row) GO.

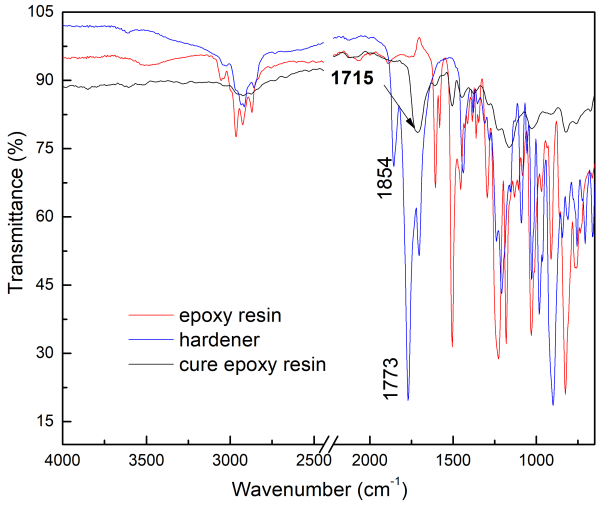

Figure 5. FTIR spectrum of bisphenol A diglycidyl ether polymer (epoxy resin), tetrahydromethylphthalic anhydride (hardener), and cured epoxy resin.

Figure 4 presents the TGA/DTG curves of the GO. The DTG curve shows the peaks of maximum temperature of mass loss. The peaks below 100°C are related to water elimination, and those between 100°C to 500°C are due to the loss of oxygen [23]. The TGA curve shows that the sum of all losses between 100°C to 500°C corresponds to 10% of the mass of GO. This result shows the low oxidation level of GO obtained in this work by the electrochemical exfoliation method, using H_2SO_4 0.5 M as electrolyte. In electrochemical exfoliation, higher oxidation levels have been achieved only at low electrolyte concentrations, near 0.2 M [24]. The major loss represents 54.6% of the mass and can be associated with the pyrolysis of the carbon framework [25].

Before studying the effect of GO on the cure kinetics of epoxy resin, we performed spectroscopy by FTIR characterization of the epoxy resin and hardener. In Figure 5, the FTIR spectra of the epoxy resin, hardener, and cured epoxy resin can be observed.

In the FTIR spectrum of the epoxy resin, the bands at 2968cm^{-1} and 2873cm^{-1} are due to methyl group C–H stretching vibration,

and at 2924cm^{-1} for methylene C–H stretching. The low-intensity band at 3052cm^{-1} is attributed to C–H stretching vibration for sp^2-hybridized carbon. The C–H in-plane bending asymmetrical vibration of methyl is observed at 1456cm^{-1}. The characteristic bands of C=C stretching of the benzene ring are observed at 1601cm^{-1}, 1583cm^{-1}, and 1510cm^{-1}. The peaks at 1235cm^{-1} and 1028cm^{-1} correspond to the C–O stretching. The characteristic absorption of C–O–C for the epoxy group is observed at 914cm^{-1} [26].

In the FTIR spectrum of the hardener, the bands at 3035cm^{-1}, 2930cm^{-1}, and 2856cm^{-1} are assigned to C–H stretching vibrations of sp^2 hybridized carbon, methylene, and methyl, respectively. The bands at 1854cm^{-1} and 1773cm^{-1} correspond to out-of-phase C=O stretching. The C=C stretching was observed at 1698cm^{-1}. At 1465cm^{-1}, the C–H in-plane bending vibration of methyl is observed. The bands at 1211cm^{-1} correspond to the C–O stretching [27].

The cure reaction is confirmed in the FTIR spectrum of the cured epoxy resin by the disappearance of bands of out-of-phase C=O stretching of the hardener and the absorption band of C–O–C for the epoxy group, and the appearance of the C=O stretching vibration band of the ester functional group (R–CO–OR') at 1715cm^{-1} [28].

Figure 6 presents the DSC curves at heating rates of 5°C/min, 10°C/min, 15°C/min, and 20°C/min for the resin studied in this research. From these data, the absolute exothermic peak temperature was obtained for each heating rate.

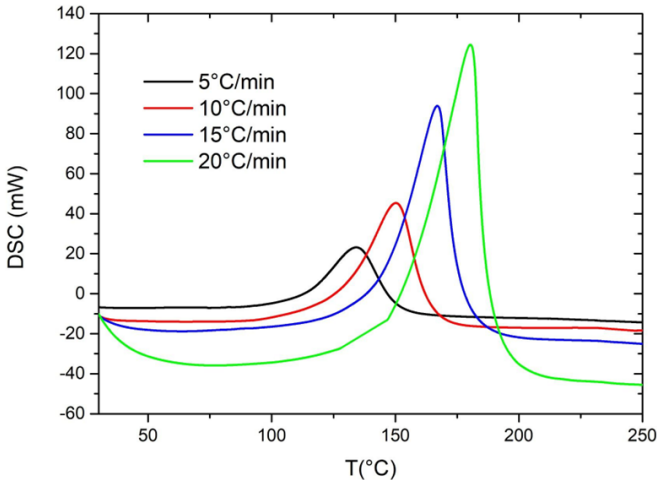

Figure 6. DSC curves for curing at different heating rates for the resin.

Table 4. Absolute temperature for each heating rate.

ϕ(°C/min)	T (°C)
5	134.18
10	150.23
15	159.20
20	167.01

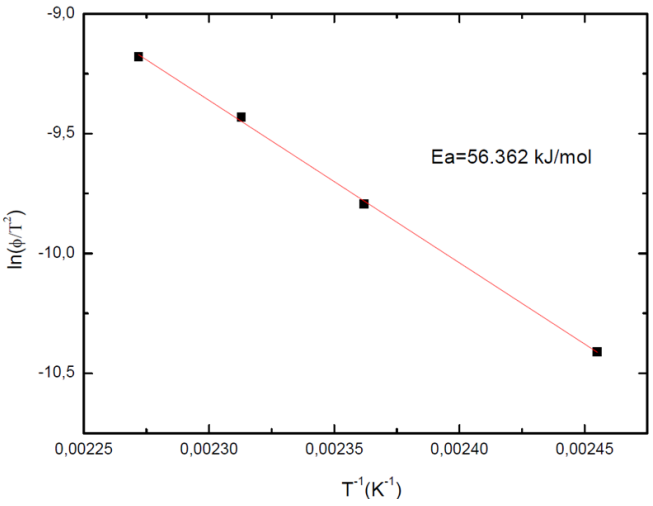

Figure 7. Values of ln(ϕ/T^2) as a function of T^{-1}, according to the equation proposed by Kissinger.

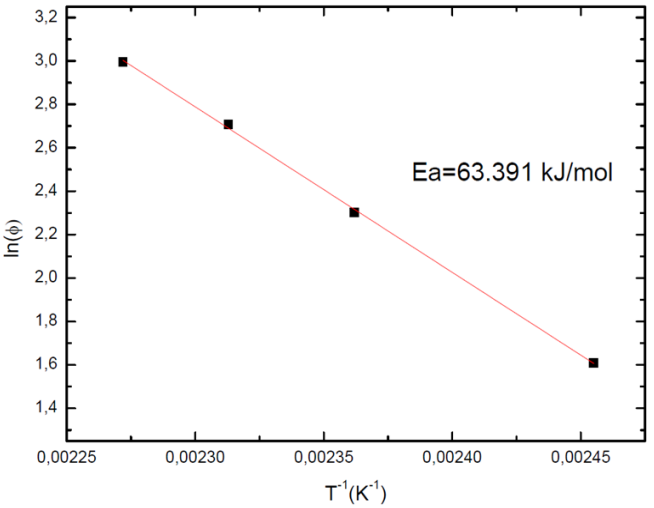

Figure 8. Values of ln(ϕ) as a function of T^{-1}, according to the equation proposed by Ozawa.

Table 4 presents the absolute temperature values corresponding to each heating rate. Based on these values and by applying the methods proposed by Kissinger and Ozawa, the activation energies for the resin analyzed in this study were determined to be Ea = 56.362 kJ/mol and Ea = 63.391 kJ/mol, respectively, as illustrated in Figures 7 and 8.

The activation energy values calculated for the studied system are close to those reported in the literature for the epoxy-anhydride system. Literature confirms that the anhydride used in this study, tetrahydromethylphthalic anhydride (ATHMF), exhibits higher activity, resulting in a lower activation energy for the epoxy/ATHMF curing process. The activity depends on the molecular structure of the anhydride; ATHMF contains unsaturated alicyclic side groups that enhance intermolecular interactions and restrict mobility, making it an active anhydride in the epoxy resin curing

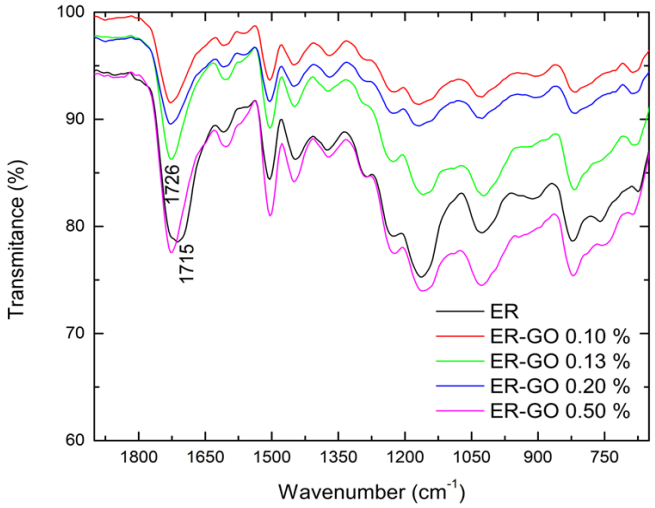

Figure 9. Comparative FTIR spectrum of EP-GO composites cured.

Table 5. Absolute temperature for each heating rate as a function of GO concentration.

GO Concetration (%)	ϕ (°C/min)	T (°K)
0.10	5	407.67
	10	423.84
	15	429.31
	20	440.17
0.13	5	408.35
	10	422.69
	15	423.34
	20	428.84
0.20	5	408.11
	10	420.58
	15	433.17
	20	432.24
0.50	5	405.63
	10	420.73
	15	430.66
	20	438.99

Table 6. Activation energy for each GO concentration calculated using the Kissinger and Ozawa methods.

GO (%)	E_a (Kissinger) (kJ/mol)	E_a (Kissinger) (kJ/mol)
0.10	56.362	63.391
0.13	89.094	96.038
0.20	66.232	73.228
0.50	54.879	61.887

reaction [29]. The curing reaction mechanism between the epoxy resin and the anhydride is well known in the literature [30]. This reaction can be catalyzed; however, as the presence of a catalyst in the hardener formulation is unknown, we present the proposed uncatalyzed mechanism.

Epoxy resin–graphene oxide composite (ER-GO) at compositions of 0wt%, 0.10wt%, 0.13wt%, 0.20wt%, and 0.50wt% of GO by weight of the epoxy resin were prepared, cured, and characterized. Figure 9 comparatively shows the FTIR spectra of the cured resins containing different GO concentrations. No significant differences in band vibrations are observed in the spectra, except for the ester band near 1715cm^{-1} in the pure cured resin, which, in the composites, undergoes a hypsochromic shift to 1726cm^{-1}. This suggests that the aromatic ring of GO, being near and adjacent to the carbonyl group, increases the conjugation of the C=O bond. Therefore, there exists a molecular interaction between GO obtained by electrochemical exfoliation and the epoxy resin–an-

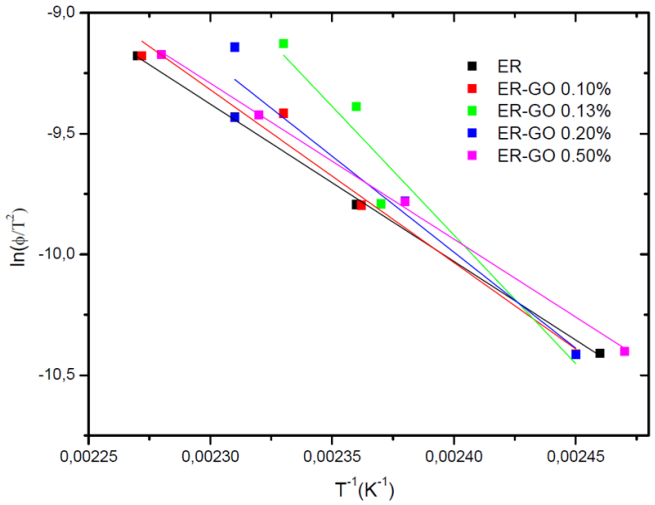

Figure 10. Kissinger Equation adjustments for different GO proportions.

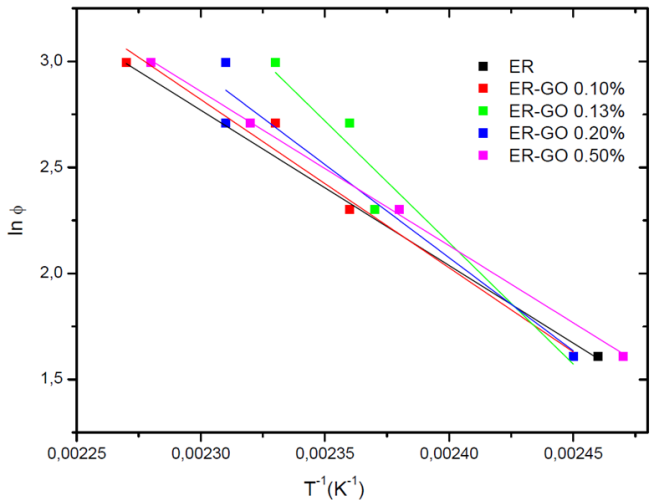

Figure 11. Ozawa Equation adjustments for different GO proportions.

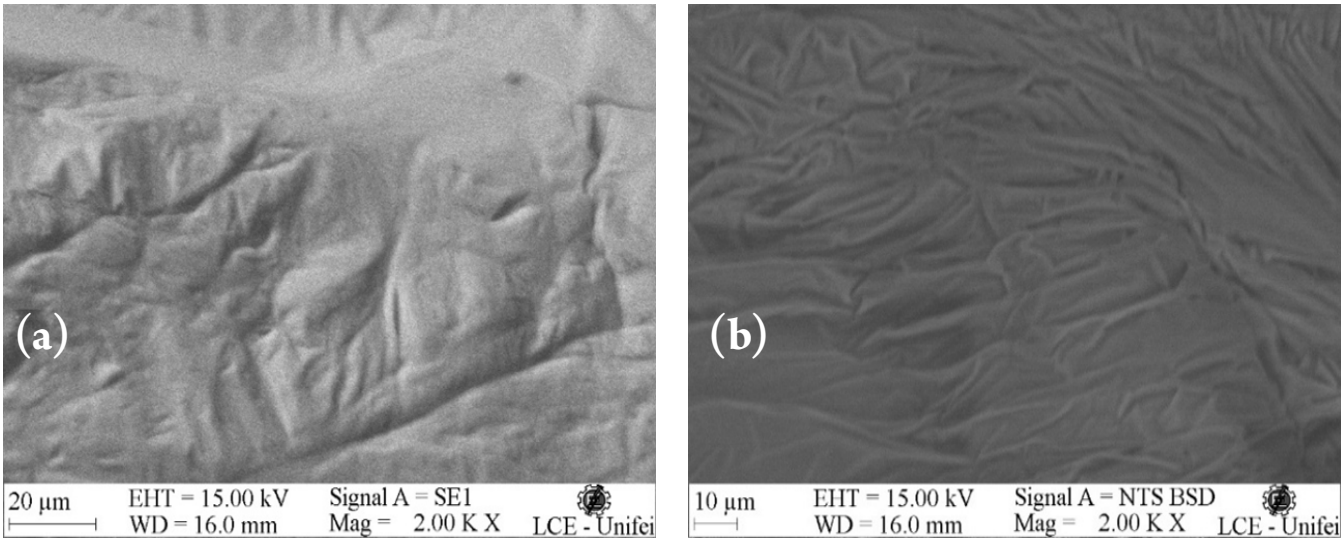

Figure 13. SEM micrograph of neat epoxy resin (a) and epoxy resin containing 0.13% GO (b).

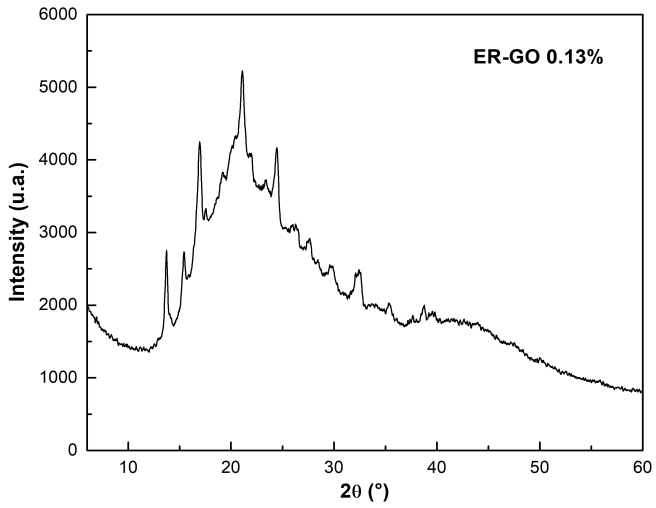

Figure 12. XRD pattern of the ER-GO 0.13% sample cured at room temperature.

hydride system.

The study of the cure kinetics of epoxy resin modified with GO was performed by Differential Scanning Calorimetry (DSC) to determine the kinetic parameters. DSC curves were obtained at the same heating rates as for the pure resin: 5°C/min, 10°C/min, 15°C/min, and 20°C/min.

Table 5 presents the absolute temperature values at each heating rate as a function of GO concentration. Based on these values and using the Kissinger and Ozawa equations, the activation energy corresponding to each GO concentration was determined.

Based on the values presented in Table 5 and applying the Kissinger and Ozawa equations, the activation energy for each GO concentration was determined. The calculated values are summarized in Table 6. Figures 10 and 11 display the curve fittings based on the Kissinger and Ozawa equations, which were used to determine the activation energies (Ea).

As shown in Table 6, there are no significant differences between the Ea determined by both kinetic methods. The low GO content of 0.10% by weight showed no difference compared to pure resin; however, the sample with 0.13% showed a significant increase in Ea. According to the literature, the presence of GO blocks molecular diffusion, hindering the curing reaction. The blockage is proportional to the GO particle size, increasing the curing reaction Ea [31].

We suggest that the decrease in Ea observed in samples containing 0.20% and 0.50% is a consequence of the segregation of stacked GO sheets. Due to the mixing process used in this work (physical mixing), only the GO fraction soluble in the resin affects the epoxy resin curing reaction. The insoluble fraction does not directly influence curing and, therefore, does not affect the curing kinetics. The observed effect is the opposite: the higher the GO content, the greater the decrease in Ea.

However, studies indicate a catalytic effect of GO at the beginning of the curing reaction, leading to a decrease in activation energy [32]. Thus, the reduction in Ea in the sample with 0.50% GO may be attributed to this catalytic effect.

The microstructural study by XDR was realized on the sample ER-GO 0.13% to check the interaction between the epoxy resin and the GO sheets. The XDR pattern of ER-GO 0.13% is shown in Figure 12.

The XRD pattern of neat epoxy is characterized by a broad peak at 2θ near 18°, related to amorphous ordering of the polymer chains [33]. The XDR pattern of ER-GO 0.13% observed in Figure 13 is represented by a synergistic response showing different reflection peaks within of broad peak. The different reflection peaks can be attributed to the formation of several structures of GO intercalated between the epoxy polymer chains [34]. This result was confirmed by the higher activation energy of the ER-GO 0.13% sample during the cure reaction of epoxy resin.

Figure 13 shows comparatively the SEM image of the surface after mechanical fracture, of ER and ER-GO 0.13% samples. The image of ER matrix revels ripple surface. The image of ER-GO 0.13% shows a homogeneous surface with a greater number of rip-

Table 7. Tg values of the composites.

DSC	Tg (°C)
ER	130.70
ER + 0.10 GO	131.40
ER + 0.13 GO	130.00
ER + 0.20 GO	131.20
ER + 0.50 GO	131.19

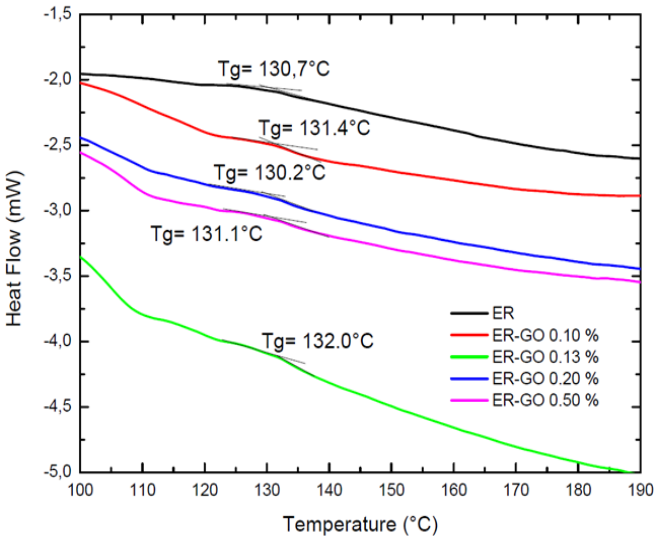

Figure 14. SEM micrograph of neat epoxy resin (a) and epoxy resin containing 0.13% GO (b).

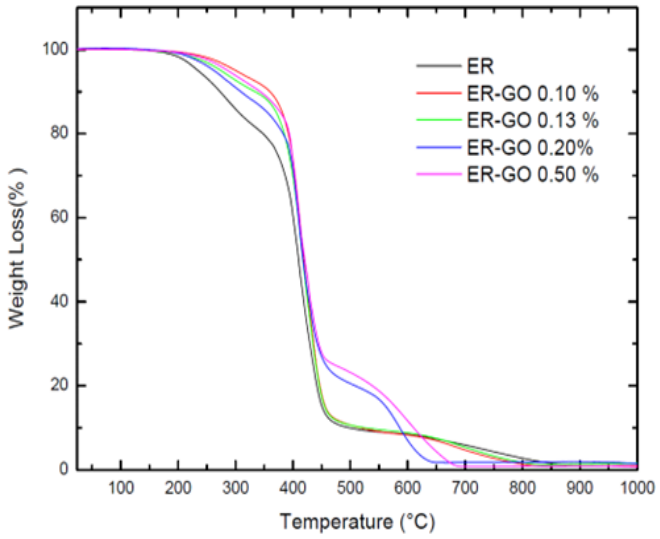

Figure 15. Comparison of the TGA results of the epoxy resin and those with different proportions of GO. The TGA analysis shows that the epoxy resin is thermally less stable than the compositesin containing 0.13% GO (b).

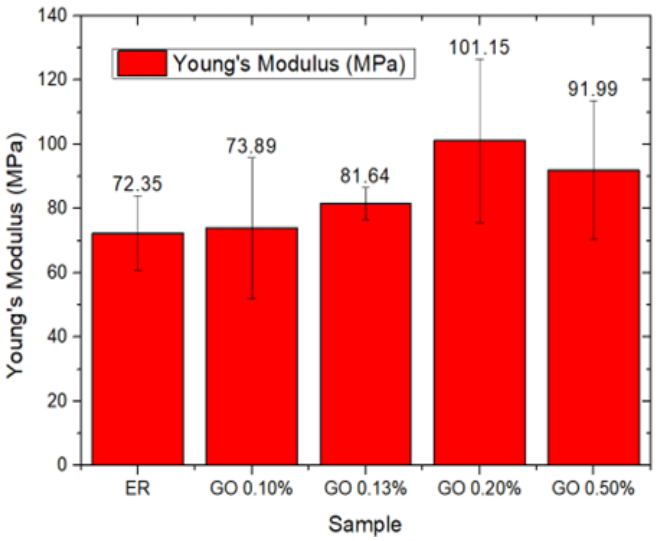

Figure 16. Young's Modulus graph of the CPs.

ples, not observed phase segregation. This result agrees with XDR pattern of ER-GO 0.13%. Also, the absence of any voids suggests good adhesion between epoxy matrix and GO. The glass-rubber transition (Tg) did not change significantly with the presence of GO, as seen in Figure 14 and Table 7.

According to the literature, the Tg of epoxy matrix composite systems depends on the synergy between curing reaction conversion and molecular confinement [35]. There is a close relationship between the degree of curing of epoxy resin and Tg. In this work, a higher Tg value was observed in the epoxy-anhydride system with higher activation energy for the cure reaction. This suggests better mixing levels between epoxy polymer chain and GO sheets in the EP-GO 0.13% sample, consequently higher confinement of GO and higher Tg. Differently, higher GO concentrations do not allow full confinement of GO, resulting in Tg values similar to epoxy resin.

Figure 15 presents the comparison of the TGA curves of the neat epoxy resin and the composites containing different proportions of GO. It is observed that the epoxy resin exhibits lower thermal stability compared to the composites. Among the samples analyzed, the one containing 0.1% GO showed the highest thermal stability, indicating that this concentration contributes most effectively to the preservation of the material's thermal properties. The ER-GO 0.2 and ER-GO 0.5% show higher thermal stability at 500°C. This region corresponds with the pyrolysis of the carbon framework of GO, as seen in Figure 4. Therefore, low concentration of GO shows higher mixing level with epoxy resin and higher initial thermal stability. Differently, higher concentration of GO shows a minor mixing level with epoxy resin, smaller initial thermal stabilization and higher end thermal stabilization. Compression tests were conducted using an Emic machine, model DL3000, and the obtained values are presented in Figure 16.

The Young´s modulus results reveal that the increase of mechanical properties of the ER-GO composite is statistically significant at concentrations of 0.2% and 0.5% of graphene oxide in the polymer matrix. Observing the error bars, we can conclude that there is no significant difference between the elastic modulus of

EP-GO 0.2% respect to EP-GO 0.5%. An increase in the elastic modulus of the epoxy matrix containing GO has been reported in the literature [36]. This behavior is often attributed to the effective dispersion and interaction between GO and the polymer matrix, especially when functionalized or doped forms of GO are used.

The results obtained from studying cured resin composites with different GO concentrations revealed significant effects on activation energy, thermal behavior, and mechanical properties. Kinetic analysis demonstrated that the activation energy varied with GO content, showing an initial increase at 0.13% GO, followed by a decrease at higher concentrations, likely due to particle segregation and possible catalytic effects. Thermal analysis indicated that the glass transition temperature (Tg) remained relatively stable across all compositions, suggesting a balance between molecular confinement and cure conversion effects. Mechanical tests showed a slight improvement in Young's modulus for the composite containing 0.20% and 0.5% GO, aligning with literature reports on reinforcement effects. Overall, the results suggest that the incorporation of GO influences the curing kinetics and mechanical performance of the epoxy matrix, with potential applications in optimizing composite formulations.

4. CONCLUSION

In The electrochemical exfoliation of graphite to obtain GO was successfully performed, as confirmed by FTIR, XRD, and SEM characterizations. FTIR spectra revealed the presence of C–O and C=O functional groups, while XRD analysis showed the characteristic diffraction peak of GO, with an interplanar spacing of 0.93 nm and an average of nine stacked layers. XRD also indicated the presence of residual graphite. The average stacking diameter of the GO phases was approximately 29.07 nm and 11.19 nm. SEM images revealed a wrinkled morphology, characteristic of stacked GO sheets, supporting the structural features expected in exfoliated GO. Spectroscopic characterization of the resin and hardener confirmed that the studied system consisted of DGEBA and ATHMF. The curing of the DGEBA–ATHMF system was verified by FTIR, where the appearance of an ester band at 1715 cm^{-1} indicated successful crosslinking. A hypsochromic shift to 1726 cm^{-1} in the ER-GO composites suggested molecular interaction between the electrochemically exfoliated GO and the epoxy–anhydride matrix.

Dynamic curing studies showed that the Ea of the pure resin was influenced by the addition of GO. At low GO concentrations, Ea increased, likely due to the blocking effect of GO on the reactions between hydroxyl–anhydride and carboxylic acid–epoxy functional groups. Conversely, at higher GO concentrations, a decrease in Ea was observed, possibly resulting from stacked GO sheet segregation and/or the catalytic effect of GO on the curing reaction. The glass transition temperature (Tg) of the composites did not exhibit significant variation compared to the pure resin. However, an increase in the elastic modulus was observed in the ER-GO composites, indicating a reinforcing effect of GO in the epoxy matrix. Among the tested samples, the one containing 0.1% GO demonstrated the highest thermal stability, suggesting that this concentration most effectively contributes to preserving the material's thermal performance.

ACKNOWLEDGEMENTS

The authors would like to thank the Brazilian agencies CAPES, CNPq and Fapemig for their financial support.

CREDIT AUTHOR STATEMENT

Maria Elena Leyva Gonzalez: Supervision, Conceptualization, Methodology, Writing-Original draft preparation, Writing-Reviewing and Editing. **Gina Maritzell Colmenares Jimenez**: Investigation, Data curation, Formal analysis, Writing-Original draft preparation. **Adhimar Flávio Oliveira**: Supervision, Conceptualization, Methodology, Writing-Original draft preparation, WritingReviewing and Editing. **Tessa Martins de Carvalho Carneiro**: Investigation, Data curation, Formal analysis. **Estacio Tavares Wanderley Neto**: Investigation, Data curation, Formal analysis

DECLARATIONS

Conflict of interest The authors declare that they have no known competing financial interests or personal relationships that could have appeared to influence the work reported in this paper.

REFERENCES

[1] Badrinath, R., & Senthilvelan, T. (2014). Comparative investigation on mechanical properties of banana and sisal reinforced polymer based composites. Procedia Materials Science, 5, 2263–2272.

[2] Ramesh, M., Palanikumar, K., & Reddy, K. H. (2014). Processing and mechanical property evaluation of banana fiber reinforced polymer composites. Procedia Engineering, 97, 563–572.

[3] Phiri, J., Gane, P. A. C., & Ndlovu, T. (2019). A review of graphene oxide in epoxy coatings: Insight into its structural, mechanical and barrier properties. Journal of Coatings Technology and Research, 16(6), 1501–1513. https://doi.org/10.1007/s11998-019-00248-1.

[4] Kim, H., Abdala, A. A., & Macosko, C. W. (2010). Graphene/polymer nanocomposites. Macromolecules, 43(16), 6515–6530. https://doi.org/10.1021/ma100572e.

[5] Rafiee, M. A., Rafiee, J., Srivastava, I., Wang, Z., Song, H., Yu, Z. Z., & Koratkar, N. (2010). Fracture and fatigue in graphene nanocomposites. Small, 6(2), 179–183. https://doi.org/10.1002/smll.200901480.

[6] Zhang, Y., Pan, C., Xu, G., & Sun, G. (2018). Improved thermal and mechanical properties of epoxy composites reinforced with graphene oxide–carbon nanotube hybrids. Composites Part A: Applied Science and Manufacturing, 112, 456–467. https://doi.org/10.1016/j.compositesa.2018.06.021.

[7] Liu, J., Li, C., & Xu, X. (2020). Study on curing behavior and properties of epoxy resin filled with electrochemically exfoliated graphene oxide. Thermochimica Acta, 689, 178632. https://doi.org/10.1016/j.tca.2020.178632.

[8] Wang, D., Li, Y., Chen, Y., Ma, M., & Wang, Z. (2022). Preparation and properties of electrochemically exfoliated graphene oxide for epoxy resin reinforcement. Journal

of Applied Polymer Science, 139(7), e51401. https://doi.org/10.1002/app.51401.

[9] Yu, W., Sisi, L., Haiyan, Y., & Jie, L. (2020). Progress in the functional modification of graphene/graphene oxide: A review. RSC Advances, 10(26), 15328–15345. https://doi.org/10.1039/D0RA01068E.

[10] Phiri, J., Günther, B., Krause, B., & Pötschke, P. (2017). General overview of graphene: Production, properties and application in polymer composites. Materials Science and Engineering: B, 215, 9–28.

[11] Yu, W., Sisi, L., Haiyan, Y., & Jie, L. (2020). Progress in the functional modification of graphene/graphene oxide: A review. RSC Advances, 10(26), 15328–15345. https://doi.org/10.1039/D0RA01068E.

[12] Pereira, E. L., Gama, A., González, M. E. L., & Oliveira, A. F. (2023). Synergistic electrochemical method to prepare graphene oxide/polyaniline nanocomposite. Polímeros: Ciência e Tecnologia, 33, 1. https://doi.org/10.1590/0104-1428.20220105.

[13] Kissinger, H. E. (1957). Reaction kinetics in differential thermal analysis. Analytical Chemistry, 29(11), 1702–1706. https://doi.org/10.1021/ac60131a045.

[14] Flynn, J. H. (1997). The 'temperature integral' - its use and abuse. Thermochimica Acta, 300(1–2), 83–92.

[15] Handayani, M., Ramadhani, R., Kurniawan, R., & Yulizar, Y. (2019). Synthesis of graphene oxide from used electrode graphite with controlled oxidation process. IOP Conference Series: Materials Science and Engineering, 541(1), 012032. https://doi.org/10.1088/1757-899X/541/1/012032.

[16] Brusko, V., Shashkova, I., Skryshevsky, V., & Orudzhev, G. (2024). Unraveling the infrared spectrum of graphene oxide. Carbon, 229, 119507. https://doi.org/10.1016/j.carbon.2024.119507.

[17] Ali, M. E. A. (2019). Preparation of graphene nanosheets by electrochemical exfoliation of a graphite–nanoclay composite electrode: Application for the adsorption of organic dyes. Colloids and Surfaces A: Physicochemical and Engineering Aspects, 570, 107–116. https://doi.org/10.1016/j.colsurfa.2019.02.063.

[18] Pereira, N. G. A., González, M. E. L., Queiroz, A. A. A., Oliveira, A. F., & Tavares Wanderley Neto, E. (2023). Higher electrical conductivity of functionalized graphene oxide doped with silver and copper (II) ions. Energies, 16, 7019. https://doi.org/10.3390/en16207019.

[19] Stobinski, L., Lesiak, B., Malolepszy, A., Mazurkiewicz, M., Mierzwa, B., Zemek, J., Jiricek, P., & Bieloshapka, I. (2014). Graphene oxide and reduced graphene oxide studied by the XRD, TEM and electron spectroscopy methods. Journal of Electron Spectroscopy and Related Phenomena, 195, 145–154. https://doi.org/10.1016/j.elspec.2014.07.003.

[20] Song, J., Wang, X., & Chang, C.-T. (2014). Preparation and characterization of graphene oxide. Journal of Nanomaterials, 2014, 276143. https://doi.org/10.1155/2014/276143.

[21] Zhu, X., Guo, Y., & Zheng, B. (2024). Graphene oxide covalently functionalized with 5-methyl-1,3,4-thiadiazol-2-amine for pH-sensitive Ga^{3+} recovery in aqueous solutions. Molecules, 29(16), 3768. https://doi.org/10.3390/molecules29163768.

[22] Sheng, Q., Yang, Y., Zhang, H., Chen, X., & Wang, X. (2024). The study of curing behavior and thermo-mechanical properties of epoxy adhesives with different anhydrides. Polymer, 307, 127342.

[23] Farivar, F., Sanchez-Rosado, A., Wu, T., & Izake, E. L. (2021). Thermogravimetric analysis (TGA) of graphene materials: Effect of particle size of graphene, graphene oxide and graphite on thermal parameters. C, 7(2), 41. https://doi.org/10.3390/c7020041.

[24] Liu, W. W., & Aziz, A. (2022). Review on the effects of electrochemical exfoliation parameters on the yield of graphene oxide. ACS Omega, 7, 33719–33731. https://doi.org/10.1021/acsomega.2c04099.

[25] Mensah, B. (2023). A systematic study of the effect of graphene oxide and reduced graphene oxide on the thermal degradation behavior of acrylonitrile-butadiene rubber in air and nitrogen media. Scientific African, 19, e01501. https://doi.org/10.1016/j.sciaf.2022.e01501.

[26] Ng, J. X. Y., Goh, K. T., Teo, C. Y., & Chan, S. Y. (2024). A study on the surface responses and degradation mechanisms of epoxy-amine coating subjected to UV accelerated weathering and hygrothermal ageing using ToF-SIMS and FTIR analysis. Polymer Degradation and Stability, 228, 110930. https://doi.org/10.1016/j.polymdegradstab.2024.110930.

[27] Salih, B. D., Mahdi, A. M., & Al-Khuzaie, A. A. (2021). Biological activity and laser efficacy of new Co (II), Ni (II), Cu (II), Mn (II) and Zn (II) complexes with phthalic anhydride. Materials Today: Proceedings, 43, 869–874. https://doi.org/10.1016/j.matpr.2020.07.083.

[28] Yang, Y., Liu, Y., & Su, Z. (2015). Thermal aging of an anhydride-cured epoxy resin. Polymer Degradation and Stability, 118, 111–119.https://doi.org/10.1016/j.polymdegradstab.2015.04.017.

[29] Alabiso, W., & Schlögl, S. (2020). The impact of vitrimers on the industry of the future: Chemistry, properties and sustainable forward-looking applications. Polymers, 12(8), 1660.

[30] Chen, X., Yang, Y., Zhang, H., & Sheng, Q. (2021). Effects of graphene oxide size on curing kinetics of epoxy resin. RSC Advances, 11(47), 29215–29226.

[31] Wang, X., Chen, X., Zhang, H., & Sheng, Q. (2016). Effect of graphene oxide sheet size on the curing kinetics and thermal stability of epoxy resins. Materials Research Express, 3(10), 105303.

[32] Víctor G. Baldovino-Medranoa, V.N.-C., Isaacs-Giraldo, R. Systematic Analysis of the Nitrogen Adsorption-Desorption Isotherms Recorded for a Series of Microporous – Mesoporous Amorphous Aluminosilicates Using Classical Methods Víctor G. Baldovino-Medrano. 2020.

[33] H.W. Wen, Z., Wang, Q., Yang, Y., Si, L. Pore Structure Characteristics and Evolution Law of Different-Rank Coal Samples. Geofluids 2021, 2021, 1–17, doi:10.1155/2021/1505306.

[34] Yao, Y., Yu, Y., Ge, D., Zhang, Y., Du, C., Ye, H., Wan, L., Chen, J., Xie, M. Nanocarbon of Moderate Microporosity Doped with Oxygenate Redox Pairs to Achieve Superior Gravimetic/Volumetric Supercapacitor Performances. Appl. Surf. Sci. 2023, 612, 155811, doi:10.1016/j.apsusc.2022.155811.

[35] Qin, Q., Wang, J., Tang, Z., Jiang, Y., Wang, L. Mesoporous Activated Carbon for Supercapacitors Derived from Coconut Fiber by Combining H3PO4-Assisted Hydrothermal Pretreatment with KOH Activation. Ind. Crops Prod. 2024,

208, 117878, doi:10.1016/j.indcrop.2023.117878.

[36] Taer, E., Apriwandi, A., Febriani, W., Taslim, R. Suitable Micro/Mesoporous Carbon Derived from Galangal Leaves (Alpinia Galanga L.) Biomass for Enhancing Symmetric Electrochemical Double-Layer Capacitor Performances. ChemistrySelect 2022, 7, e202201810, doi:10.1002/slct.202201810.